Journal of Crystal Growth 315 (2011) 242–245

Contents lists available at ScienceDirect

Journal of Crystal Growth

journal homepage: www.elsevier.com/locate/jcrysgro

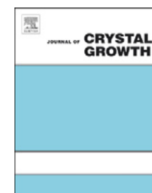

Study of the internal quantum efficiency of InGaN/GaN UV LEDs on patterned sapphire substrate using the electroluminescence method

C.H. Wang [a], C.C. Ke [a], C.H. Chiu [a], J.C. Li [a], H.C. Kuo [a,*], T.C. Lu [a,b], S.C. Wang [a]

[a] Department of Photonics and Institute of Electro-Optical Engineering, National Chiao Tung University, 1001 University Road, Hsinchu 30050, Taiwan
[b] Institute of Lighting and Energy Photonics, National Chiao Tung University, 301 Gaofa 3rd Road, Guiren Township, Tainan County 711, Taiwan

ARTICLE INFO

Available online 24 September 2010

Keywords:
A1. Substrates
A3. Metalorganic chemical vapor deposition
B1. Nitrides
B3. Light emitting diodes

ABSTRACT

Internal quantum efficiency (IQE) of InGaN/GaN UV LEDs with patterned sapphire substrates (PSS) was investigated using electroluminescence (EL) and photoluminescence (PL) methods. The physical mechanisms that affect temperature-dependent EL efficiency as a function of injected carrier density were deduced. In order to reduce the density of non-radiative recombination centers to improve quantum efficiency, improvement of crystal quality and reduction in the number of defects are necessary. PSS LEDs showed better EL characteristics than non-PSS LEDs because of the improved epitaxial quality. Contrary to PL IQE, EL IQE was significantly affected by carrier injection efficiency, especially at low temperature when high bias voltage was applied to the p–n junction.

Crown Copyright © 2010 Published by Elsevier B.V. All rights reserved.

1. Introduction

III-nitride based light emitting diodes (LEDs) have attracted much attention for green to ultraviolet (UV) wavelengths in the last decade due to the tunable wide band gap. Recently, LEDs in the UV range have been the focus of research because of their tremendous potential in applications like white light sources [1], environmental cleaning, and bio-medical examination. It is well known that high efficiency radiative recombination in blue and green InGaN multiple quantum wells LEDs has been mainly attributed to the localized states due to phase separation or fluctuations in In mole fraction in $In_xGa_{1-x}N$/GaN quantum wells [2]. For UV LEDs, InN mole fraction in the InGaN well is lower than that for blue or green LEDs, so the radiative efficiency of such LEDs is more sensitive to the threading dislocation density.

Some research groups have investigated the temperature dependence of electroluminescence (EL) intensity of InGaN/GaN QW diodes [3,4], which reveals anomalous EL quenching at temperatures below 100 K. It was found that the anomalous temperature dependence of EL efficiency is caused by the interplay of radiative recombination in QWs and the carrier injection coefficient. One of the anticipated genuine causes for low temperature EL quenching may be ascribed to the deep Mg acceptor level of 170 meV in p-GaN [5], which can be deactivated at lower temperatures below 100 K. Therefore, holes fail to be injected into the QW active region from the p-GaN layer, especially when an electron blocking p-type AlGaN barrier is introduced.

Moreover, although the external quantum efficiency (EQE) of UV LEDs grown on patterned sapphire substrate (PSS) can be significantly improved due to the low dislocation density and high extraction efficiency (η_{lee}), the actual enhancement in IQE and η_{lee} is still hard to quantify. In this study, we analyzed the detailed physical mechanisms for EL enhancement effects under forward bias conditions, and the effects of dislocation density in UV LEDs were also examined. EL behavior under low and high injection current is investigated from low temperature (LT) to room temperature (RT). The EL IQE results were compared to photoluminescence (PL) IQE results to investigate the difference between these methods.

2. Experiments

The etched patterns on sapphire substrate are 2D arrays of holes arranged in a hexagonal lattice with depth 1.4 μm and diameter 3.5 μm, and the distance between each pattern is 1.0 μm. The detailed process can be found in Ref. [6]. The LED structure was then grown on a planar substrate and PSS by low-pressure metal–organic chemical vapor deposition.

The epitaxial structure consisted of a 30-nm-thick AlN nucleation layer, a 2-μm-thick Si-doped n-type GaN, and an unintentionally doped active layer with $In_xGa_{1-x}N$/GaN MQWs, a 20-nm-thick $Al_xGa_{1-x}N$ electron blocking layer, and a 0.2-μm-thick Mg-doped p-type GaN. The doping concentrations of n- and p-type GaN were nominally 5×10^{18} and $1\times10^{19}\,cm^{-3}$,

* Corresponding author. Tel.: +886 3 571 2121x31986; fax: +886 5 571 6631.
E-mail address: hckuo@faculty.nctu.edu.tw (H.C. Kuo).

0022-0248/$ - see front matter Crown Copyright © 2010 Published by Elsevier B.V. All rights reserved.
doi:10.1016/j.jcrysgro.2010.09.046

respectively. The MQW comprised 16 periods of an $In_{0.15}Ga_{0.85}N$ well (~2 nm) and a GaN barrier (~16 nm), and the emission wavelength of both samples is around 400 nm at 20 mA. The LEDs were fabricated through the standard process, and the size of LED mesas was 300 × 300 μm^2.

For the temperature-dependent EL measurement, the sample was mounted in a closed-cycle helium cryostat and temperature was controlled from 15 to 300 K. Output light was detected by a 0.32 m monochromator (Jobin-Yvon Triax-320) with 1800, 1200, and 300 grooves/mm gratings and the maximum width of the entrance slit was 1 mm. The injection current was from 0.1 to 80 mA, which can be calculated in terms of current density as from 0.11 to 88 A/cm^2. The details of the temperature-dependent EL measurement setup are shown in Fig. 1. PL was excited by a femto-second-pulse Ti:Sapphire laser whose output wavelength could be tuned to be around 380–390 nm to avoid absorption by GaN and ensure that most of the photons generated by the laser light could excite the photons in the MQWs. Details of the PL IQE measurement and the definition of injected carrier density were published in Ref. [7].

3. Results and discussion

The temperature-dependent relative IQE curves versus injection current are summarized in Fig. 2(a) and (b), for the PSS and non-PSS LEDs, respectively. We define the relative IQE as the output power collected from the LED divided by the injection current. Generally, EQE can be defined as the product of η_{lee} and IQE. Since precise η_{lee} is hard to accurately measure and separate from IQE, we use normalization to eliminate η_{lee}, which is almost constant under various temperatures and injection currents. For every specific condition, the maximum efficiency is set as 1 to normalize others. At first glance, one could find that at every temperature, as the injection current increased, there is a peak efficiency. However, this peak position varied as temperature changed. For example, it was around 8 mA when temperature was above 120 K and gradually moved to 1 mA when temperature decreased to 80 K. Moreover, the maximum in all the measurement curves happened at around 80 and 100 K for PSS LED and non-PSS LED, respectively, instead of the lowest temperature. To understand this phenomenon, further investigation is needed.

Fig. 3(a) and (b) shows the temperature-dependent relative IQE at 0.1 and 20 mA, respectively. It can clearly be seen that at the low injection current of 0.1 mA, relative EL efficiencies for both PSS and non-PSS LEDs decrease monotonously with increase in temperature. But at the injection current of 20 mA, EL efficiency first increases and then decreases with increase in temperature.

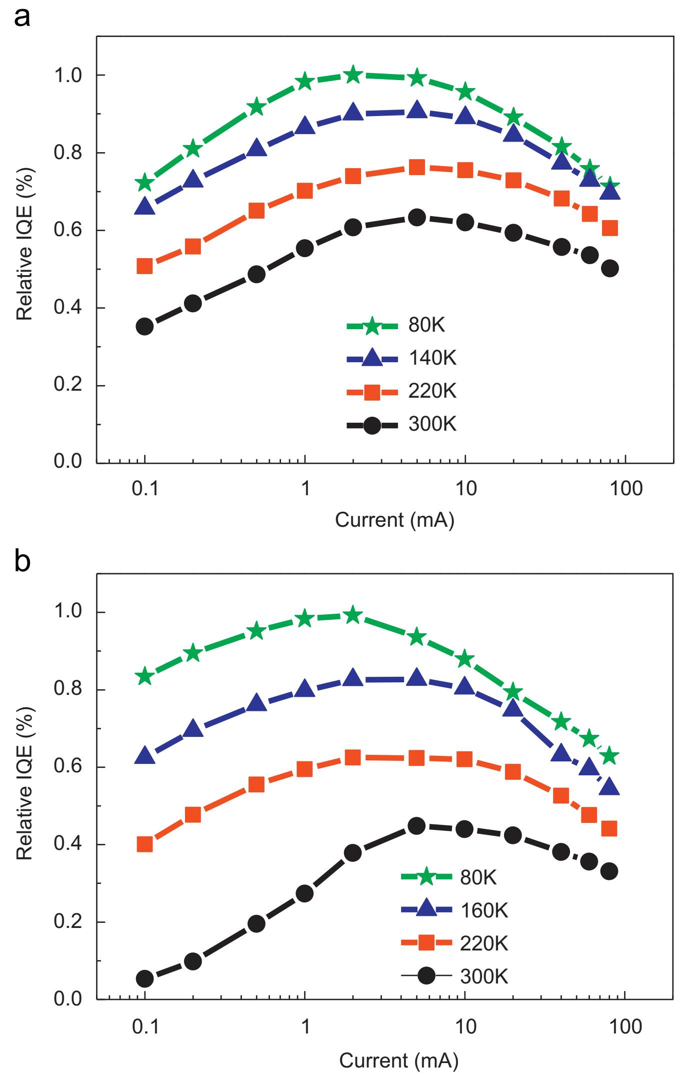

Fig. 2. Temperature-dependent relative IQE curves of (a) PSS and (b) non-PSS LEDs.

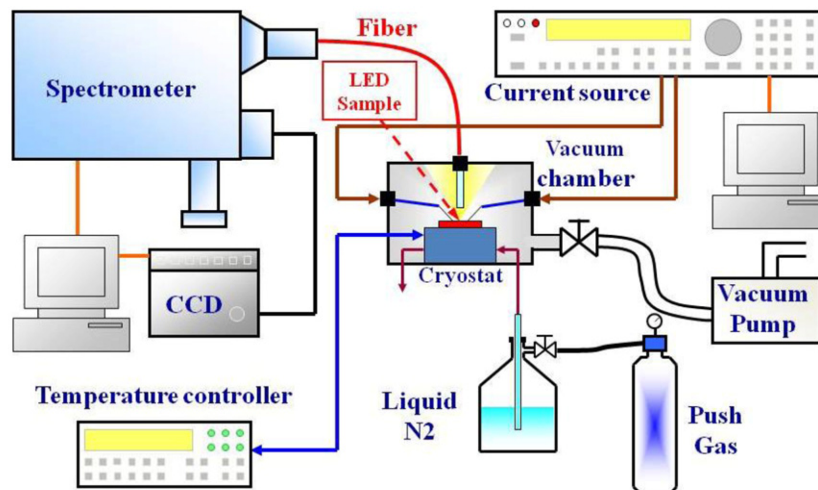

Fig. 1. Schematic of electroluminescence measurement setup.

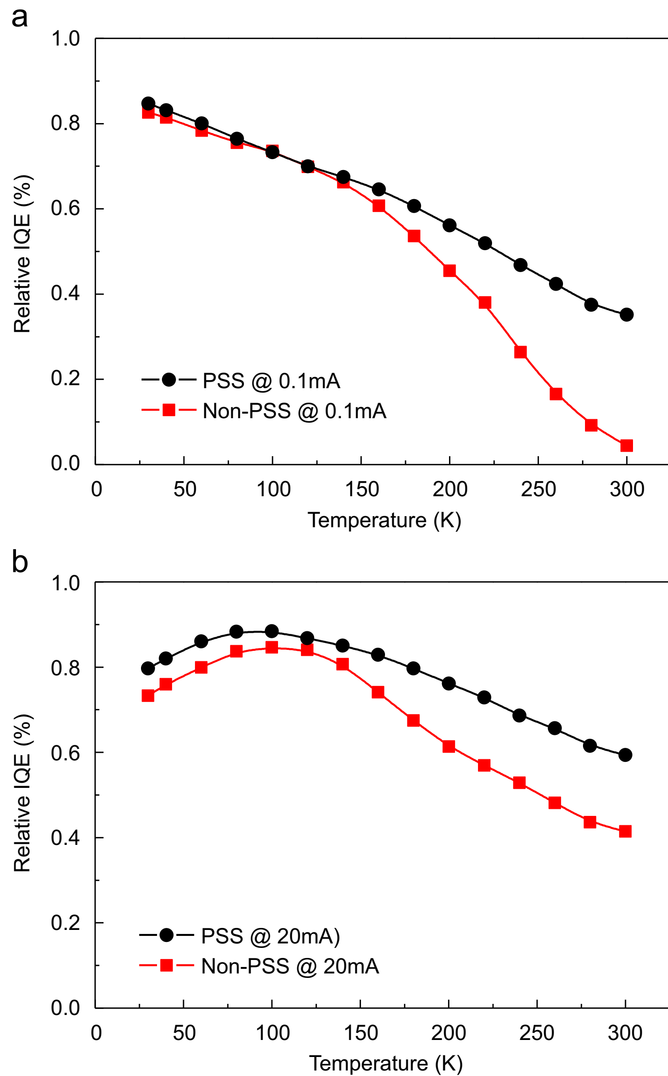

Fig. 3. Temperature-dependent relative IQE of PSS and non-PSS LEDs at (a) 0.1 mA and (b) 20 mA.

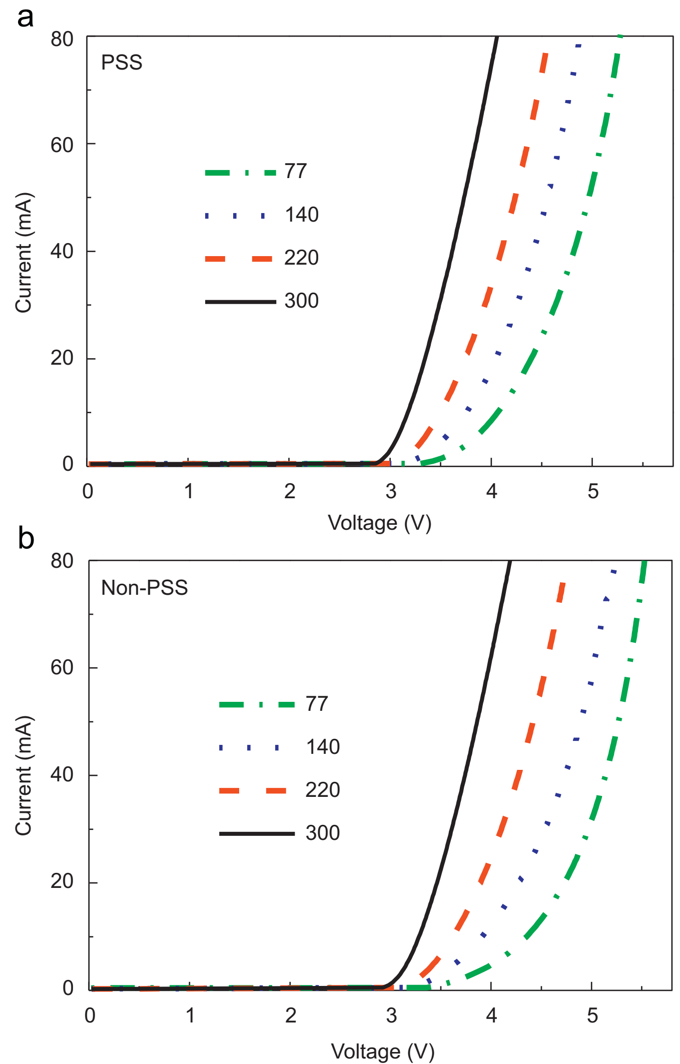

Fig. 4. Temperature-dependent *I–V* curves of (a) PSS and (b) non-PSS LEDs.

It is worth noting that EL efficiency for the PSS LED is much higher than that of non-PSS LED when temperature is above 150 K at both low and high injection currents. There are two possible mechanisms at play with increasing temperature. Firstly, in InGaN-based structures, emission comes from the localized states, which can trap carriers within their potential minima. When temperature increases, the carriers receive thermal energy and will be activated from potential minima to non-radiative centers. Therefore, EL efficiency will decrease. In the following, this is denoted as carrier delocalization effect. Secondly, it is well known that hole concentration and mobility decrease when temperature decreases, leading to increase in series resistance and forward voltage [8]. That is to say, the external field applied on the LED structure is much higher at low temperature, which will result in more carriers escaping out of the well region as well as a decrease in radiative recombination rate. In the following, this is denoted as external field effect.

To figure out which mechanism is dominant at different injection currents, we investigated the temperature-dependent *I–V* curves, as shown in Fig 4(a) and (b). At an injection current of 20 mA, the forward voltage increases by about 1 and 1.4 V from 300 to 77 K for PSS and non-PSS LEDs, respectively, while at an injection current of 0.1 mA, the variation in forward voltage is much smaller for both LEDs (only about 0.5 V). These results

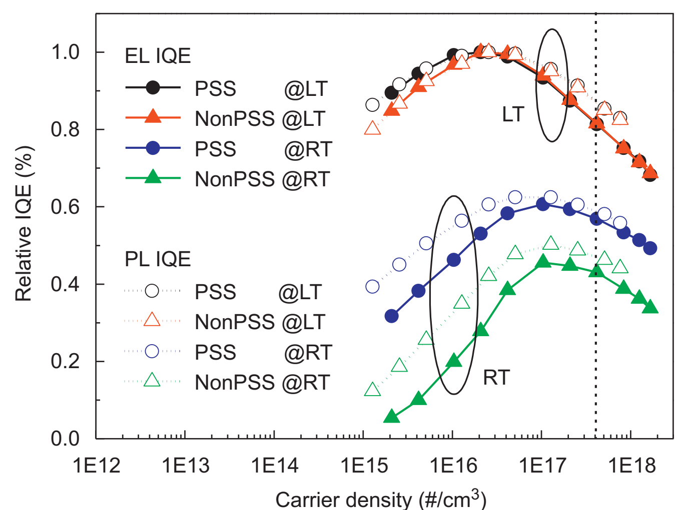

Fig. 5. Relative electroluminescence and photoluminescence IQE as a function of injection current at low temperature and room temperature.

indicate that the external field effect plays a more important role at high injection current. Therefore, we can summarize that at low injection current, the decrease in EL efficiency with increase in

temperature is mainly due to the carrier delocalization effect. But at high injection current, due to the competition of carrier delocalization effect and external field effect, EL efficiency reaches a maximum value at higher temperature. On the other hand, as temperature was decreased from 300 to 77 K, the turn-on voltages of PSS and non-PSS LEDs were increased from 2.98 to 3.74 V and 3.11 to 4.02 V, respectively. This phenomenon indicates that carrier injection in the diodes is more difficult at low temperature.

Furthermore, we compared the relative EL IQE with PL IQE as a function of carrier density at low and room temperature as shown in Fig. 5. In PL IQE measurements, since PL efficiency was almost constant for temperatures below 30 K, here we used 15 K as LT, and for EL IQE, we chose 77 K as the LT since the maximum relative IQE occurred at about 77 K. The definition of carrier density in EL measurement is the injected carrier divided by the active volume, while in PL measurement, we adopted the method in Ref. [7].

The relative PL IQE is higher than the relative EL IQE at low carrier density. This phenomenon indicates that more carrier leakage happens when carriers are injected using a current source, which causes non-uniform distribution of holes. We found that EL efficiency decreased more rapidly at high injected carrier density. This can be attributed to the forward voltage increasing with increasing injected carrier density. Since the injected electrons inefficiently recombined with holes, they easily reached the p-GaN layer, resulting in EL efficiency drooping more rapidly at LT than RT. Efficiency at RT measured by the EL method is slightly lower than that measured by PL. These results imply that EL efficiency is significantly affected by carrier injection efficiency. To increase EL efficiency, a better LED chip or epitaxial structure design might be required.

In addition, the reduction of efficiency after the maximum in the curves is the well-known efficiency droop behavior, which can be attributed to carrier overflow [9], non-uniform distribution of holes [10,11], Auger scattering [12], and carrier delocalization [13]. Comparing EL efficiency at RT with the maximum efficiency at LT, the relative IQE of the PSS LED (59.3%) is much higher than that of the non-PSS LED (42.3%) at 20 mA. However, the reduction of relative IQE with increasing injection current is almost the same in both LEDs. These results imply that the reduction of dislocation density effectively improves the efficiency but does not affect the efficiency droop behavior at high injection current, which is consistent with the results in Ref. [14].

4. Conclusion

From our analysis, we deduced the physical mechanisms that affect the temperature dependence of EL efficiency as a function of injected carrier density. The non-radiative recombination centers and the carrier overflow mechanisms both play important roles in the variation of the quantum efficiency. In order to reduce the density of non-radiative recombination centers to improve the quantum efficiency at low injected carrier density, improvement of crystal quality and reduction in density of defects are necessary. Indeed, an LED grown on PSS substrate shows higher efficiency than an LED grown on non-PSS substrate. Finally, we compared EL IQE with PL IQE. EL IQE was found to be smaller than PL IQE, which indicates that to equilibrate EL and PL IQE, carrier injection efficiency and the effect of temperature cannot be ignored.

Acknowledgments

The authors would like to thank Epistar Corporation for their technical support. This work was funded by the National Science Council in Taiwan under Grant number NSC98-3114-M-009-001.

References

[1] Y. Narukawa, I. Niki, K. Izuno, M. Yamada, Y. Murazaki, T. Mukai, Jpn. J. Appl. Phys. 41 (2002) L371.
[2] Y. Narukawa, Y. Kawakami, M. Funato, Sz. Fujita, S. Fujita, S. Nakamura, Appl. Phys. Lett. 70 (1997) 981.
[3] A. Hori, D. Yasunaga, A. Satake, K. Fujiwara, Appl. Phys. Lett. 79 (2001) 3723.
[4] C.L. Yang, L. Ding, J.N. Wang, K.K. Fung, W.K. Ge, H. Liang, L.S. Yu, Y.D. Qi, D.L. Wang, Z.D. Lu, K.M. Lau, J. Appl. Phys. 98 (2005) 023703.
[5] S. Grzanka, G. Franssen, G. Targowski, K. Krowicki, T. Suski, R. Czemecki, P. Perlin, M. Leszczyski, Appl. Phys. Lett. 90 (2007) 103507.
[6] J.H. Lee, J.T. Oh, J.S. Park, J.W. Kim, Y.C. Kim, J.W. Lee, H.K. Cho, Phys. Status Solidi C 3 (2006) 2169.
[7] C.H. Ya-Ju Lee, P.C. Chiu, T.C. Lin, H.C. Lu, Kuo, S.C. Wang, IEEE J. Sel. Top. Quantum Electron. 15 (2009) 1137.
[8] X.A. Cao, S.F. LeBoeuf, IEEE Trans. Electron Devices 54 (2007) 3414.
[9] K.J. Vampola, M. Iza, S. Keller, S.P. DenBaars, S. Nakamura, Appl. Phys. Lett. 94 (2009) 061116.
[10] K. Ding, Y.P. Zeng, X.C. Wei, Z.C. Li, J.X. Wang, H.X. Lu, P.P. Cong, X.Y. Yi, G.H. Wang, J.M. Li, Appl. Phys. B 97 (2009) 465.
[11] C.H. Wang, J.R. Chen, C.H. Chiu, H.C. Kuo, Y.L. Li, T.C. Lu,and, S.C. Wang, IEEE Photon. Technol. Lett. 22 (2010) 236.
[12] A. David, M.J. Grundmann, Appl. Phys. Lett. 96 (2010) 103504.
[13] B. Monemar, B.E. Sernelius, Appl. Phys. Lett. 91 (2007) 181103.
[14] A. Hori, D. Yasunaga, A. Satake, K. Fujiwara, Appl. Phys. Lett. 91 (2007) 231114.